Back-reaction effects of quantum vacuum in cavity quantum electrodynamics

I. Carusotto,[1,*] S. De Liberato,[2] D. Gerace,[3] and C. Ciuti[2]

[1]*INO-CNR BEC Center and Dipartimento di Fisica, Università di Trento, I-38123 Povo, Italy*

[2]*Laboratoire Matériaux et Phénomènes Quantiques, Université Paris Diderot-Paris 7 and CNRS, UMR 7162, 75205 Paris Cedex 13, France*

[3]*Dipartimento di Fisica "A. Volta" and UdR CNISM, Università di Pavia, I-27100 Pavia, Italy*

(Received 3 July 2011; published 7 February 2012)

We theoretically study an optical system in which the back-reaction of quantum vacuum manifests itself as a sizable suppression of the absorption by a three-level emitter embedded in an optical cavity. A theoretical model including the anti-rotating-wave terms of the light-matter interaction Hamiltonian is developed to describe the conversion of zero-point fluctuations into observable radiation, as well as the back-reaction of the quantum vacuum onto the emitter.

DOI: 10.1103/PhysRevA.85.023805 PACS number(s): 42.50.Pq, 03.70.+k, 42.50.Ct, 42.50.Lc

I. INTRODUCTION

One of the most intriguing predictions of quantum mechanics is the existence of significant field fluctuations in the ground state of a quantum field theory; as a result, the quantum vacuum is not just an empty void but has a nontrivial structure. The zero-point quantum fluctuations of the electromagnetic field, in particular, are responsible for a number of observable effects, from spontaneous emission and Lamb shift in atomic physics to the Casimir force between neutral objects [1].

A further fascinating prediction of quantum field theory is the conversion of the zero-point fluctuations of a quantum field into pairs of real particles when the boundary conditions of the field are varied in time at a fast-enough rate, the so-called dynamical Casimir effect (DCE) [2–4]. In the simplest and most celebrated version, a DCE emission with peculiar spectral properties has been predicted to occur when a plane metallic mirror is moving through the electromagnetic vacuum with a nonuniform acceleration. The energy of the radiated photons comes at the expense of the mechanical energy of the moving mirror, which then experiences a friction force by the quantum vacuum via the so-called *back-reaction* effect [5].

So far, experimental observation of the DCE and, *a fortiori*, of the back-reaction force has been hindered by the extremely weak intensity that is expected for realistic experimental configurations. For this reason, researchers have started investigating a broader class of DCE-like effects that occur in the presence of generic time modulations of the optical length of a cavity, not necessarily due to a mechanical motion of the cavity mirrors. In particular, sizable DCE emission intensities have been anticipated to appear when the refractive properties of the cavity material are varied in time at a fast enough rate. Following the first proposal [6], the properties of such an analogous DCE emission have been investigated for a number of different systems [7–13]. Very recently, a first claim of experimental observation of such an analog DCE emission has been reported using a circuit QED system in the microwave range [14]. On the other hand, we are not aware of any experimental nor theoretical study of back-reaction effects in analog DCE systems.

In the present work, we take advantage of the extreme precision and flexibility of optical techniques to propose an all-optical route to observe the quantum vacuum back-reaction effect in a cavity-QED system. Inspired by recent experiments [15], we consider a specific configuration consisting of an optical cavity strongly coupled to a three-level emitter: Rabi oscillations in the emitter illuminated by a strong resonant laser drive result in a periodic modulation of the effective optical length of the cavity and, in turn, in the conversion of quantum fluctuations into observable DCE radiation. The optical analog of the friction force exerted by the quantum vacuum onto the moving mirrors manifests itself here as a sizable suppression of the absorption experienced by the laser beam driving the Rabi oscillations.

The structure of the article is the following. In Sec. II, we introduce the physical system and the theoretical model used for its description. Specific attention is paid to the theoretical issues that arise when the anti-rotating-wave terms of the light-matter interaction Hamiltonian are included in the model. This model is then used in Sec. III to predict and characterize the spectral properties of the quantum vacuum emission. The back-reaction effect of the quantum vacuum is discussed in Sec. IV. Conclusions are finally given in Sec. V.

II. THE MODEL

We start by introducing the theoretical model to describe a generic three-level optical emitter in a ladder configuration strongly coupled to an optical cavity. The level scheme we are considering is sketched in Fig. 1(a): Very recently, a configuration of this kind has been experimentally realized using a combination of interband and intersubband transitions in a semiconductor device [15]. In the near future, we expect that it can be also implemented using atoms in microwave cavities [16], Josephson qubits in superconducting circuits [14,17], or quantum dots in photonic crystal cavities [18]. An interesting theoretical study of quantum dynamics in these systems recently appeared in [19].

A. The isolated system Hamiltonian

In contrast to most existing literature on cavity QED [16,19], a correct description of the zero-point fluctuations

*carusott@science.unitn.it

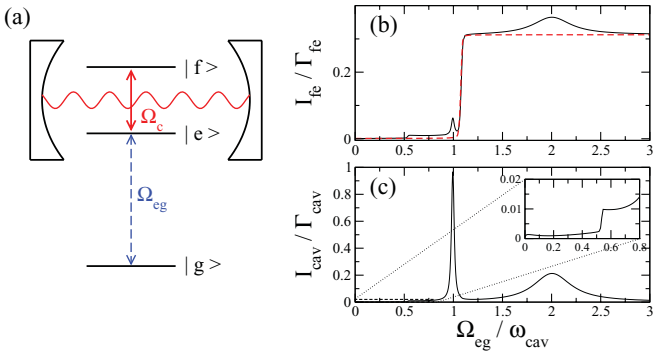

FIG. 1. (Color online) (a) Sketch of the ladder level configuration in the emitter coupled to the cavity and the optical fields driving the transitions. Right panels: total emission intensities $I_{\rm cav}$ and I_{fe} as a function of the Rabi frequency Ω_{eg} of the drive laser (solid lines). Red dashed line in panel (b): Same curve in the vanishing emitter-cavity coupling case $\Omega_{\rm cav}=0$. Within the RWA, both $I_{{\rm cav},ge}$ would be exactly zero. The chosen parameters $\omega_e-\omega_g=\omega_L$, $\omega_f-\omega_e=\omega_{\rm cav}$, $\Omega_{\rm cav}/\omega_{\rm cav}=0.1$, $\Gamma_{eg}/\omega_{\rm cav}=0.01$, and $\Gamma_{\rm cav}=\Gamma_{fe}=10^{-3}\,\omega_{\rm cav}$ correspond to a strong (but not ultrastrong) coupling regime.

requires going beyond the standard rotating-wave approximation (RWA). For our specific configuration, this can be done using a Hamiltonian of the form

$$\begin{aligned}H=&\hbar\omega_{\rm cav}\hat a^\dagger\hat a+\hbar\omega_g|g\rangle\langle g|+\hbar\omega_e|e\rangle\langle e|+\hbar\omega_f|f\rangle\langle f|\\&+\hbar\Omega_{eg}\,e^{-i\omega_L t}|e\rangle\langle g|+\hbar\Omega_{eg}\,e^{i\omega_L t}\,|g\rangle\langle e|\\&+\hbar\Omega_{\rm cav}[|f\rangle\langle e|+|e\rangle\langle f|][\hat a^\dagger+\hat a].\end{aligned}\tag{1}$$

Here, $\hbar\omega_{g,e,f}$ are the energies of the g,e,f atomic levels. The $g\leftrightarrow e$ transition is optically driven by a coherent laser of frequency ω_L and (real and positive) Rabi frequency Ω_{eg}. The anti-RWA terms of the light-emitter coupling on the $g\leftrightarrow e$ transition can be safely neglected under the assumption that the transition frequency $\omega_e-\omega_g$ is much larger than all other frequency scales.

A single cavity mode of frequency $\omega_{\rm cav}$ and destruction (creation) operator $\hat a$ ($\hat a^\dagger$) is considered, which is strongly coupled to the $e\to f$ transition with a (real and positive) vacuum Rabi frequency $\Omega_{\rm cav}$. In order to correctly describe the quantum vacuum emission, one has to go beyond the standard RWA description of cavity-QED systems [16,19] and include all terms of the emitter-cavity coupling, in particular the anti-RWA ones where a cavity photon is emitted while the atom climbs from the e to the f state and vice versa. In the following, we restrict our attention to the resonant case with $\omega_L=\omega_e-\omega_g$ and $\omega_{\rm cav}=\omega_f-\omega_e$. As required by the strong light-matter coupling regime, the light-matter coupling $\Omega_{\rm cav}$ is assumed to be much larger than all decay rates.

Thanks to the RWA assumption on the $g\leftrightarrow e$ transition, we can apply the unitary rotation operator $R(t)=e^{-i\omega_L t\,|g\rangle\langle g|}$ and move to a rotating frame where the Hamiltonian has a time-independent form:

$$\begin{aligned}H=&\hbar\omega_{\rm cav}\hat a^\dagger\hat a+\hbar(\omega_g+\omega_L)|g\rangle\langle g|+\hbar\omega_e|e\rangle\langle e|\\&+\hbar\omega_f|f\rangle\langle f|+\hbar\Omega_{eg}[|e\rangle\langle g|+|g\rangle\langle e|]\\&+\hbar\Omega_{\rm cav}[|f\rangle\langle e|+|e\rangle\langle f|][\hat a^\dagger+\hat a].\end{aligned}\tag{2}$$

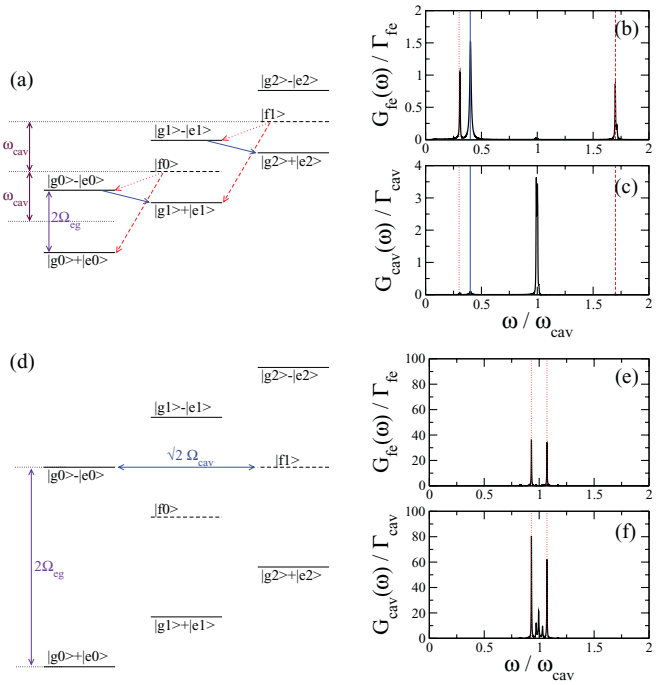

FIG. 2. (Color online) Left panels: Sketches of the dressed levels of the optically driven emitter as predicted by the Hamiltonian (2). The labels indicate the dominant contribution of each eigenstate in the weak atom-cavity coupling $\Omega_{\rm cav}$ limit. Right panels: spectra of the spontaneous emission on the $f\leftrightarrow e$ transition [(b) and (e)] and of the cavity emission [(c) and (f)]. Upper and lower group of panels [(a) and (c)] and [(d) and (f)] refer to the $\Omega_{eg}/\omega_{\rm cav}=0.7,2$ cases, respectively. Same system parameters as in Fig. 1.

The structure of the resulting eigenstates of the cavity-emitter system optically dressed by the drive laser is shown in Figs. 2(a) and 2(d) for different values of Ω_{eg}. The labels of the eigenstates refer to the dominating component in the weak $\Omega_{\rm cav}$ limit, in which the energy of the $|gn\rangle\pm|en\rangle$ and $|fn\rangle$ eigenstates are $n\omega_{\rm cav}\mp\Omega_{eg}$ and $(n+1)\omega_{\rm cav}$ respectively. In the shorthand $|jn\rangle$, n and $j=\{g,e,f\}$ respectively indicate the number of cavity photons and the state of the emitter.

B. The nonwhite dissipation baths

In addition to the CW driving laser, the system is coupled to the external world via spontaneous emission processes on the $e\to g$ and $f\leftrightarrow e$ transitions (the $f\to g$ transition is assumed to be forbidden), as well as via direct light emission from the cavity through the imperfectly reflecting mirrors. Such dissipation processes are included in the model at the level of the master equation for the density matrix ρ,

$$\frac{d\rho}{dt}=-\frac{i}{\hbar}[H,\rho]+\mathcal{L}_{eg}[\rho]+\mathcal{L}_{fe}[\rho]+\mathcal{L}_{\rm cav}[\rho].\tag{3}$$

Thanks to the large value of $\omega_e-\omega_g$, the standard RWA approximation can be performed on the $e\to g$ spontaneous emission terms, which leads to a dissipation superoperator in the usual Lindblad form [20],

$$\mathcal{L}_{eg}[\rho]=\tfrac{1}{2}\Gamma_{eg}[2\sigma_{eg}^-\rho\sigma_{eg}^+-\sigma_{eg}^+\sigma_{eg}^-\rho-\rho\sigma_{eg}^+\sigma_{eg}^-],\tag{4}$$

in both the stationary and rotating frames, with $\sigma_{eg}^{+} = |e\rangle\langle g|$ and $\sigma_{eg}^{-} = (\sigma_{eg}^{+})^{\dagger}$. In spite of this formal similarity, it is worth remembering that energy conservation shows peculiar features when seen in the rotating frame of the dressed Hamiltonian (2): As the emission spectrum on the $e \to g$ transition is shifted downward by ω_L, the sidebands on the red side of $\omega_L = \omega_e - \omega_g$ have a negative energy in the rotating frame; on the dressed-level scheme of Figs. 2(a) and 2(d), these transitions then appear to climb up the energy ladder.

The description of spontaneous emission processes on the $f \leftrightarrow e$ transition and of the cavity emission requires more care to be consistent with the anti-RWA terms of the emitter-cavity coupling in Hamiltonian (1). On one hand, one has to include anti-RWA terms also in the coupling to the dissipation baths, which allows for quite counterintuitive optical processes, for instance, the emitter going up from the e to the f state while emitting a photon by spontaneous emission. On the other hand, unphysical *perpetuum mobile* behaviors are avoided by carefully modeling the frequency-dependent density of states $v(\omega)$ of the dissipation baths.

In the present work, all baths are assumed to be zero-temperature ones, so that energy can only be dissipated from the system into them. This imposes $v(\omega) = 0$ for $\omega < 0$. For the numerical calculations shown in the figures, specific model forms of $v_j(\omega)$ have been considered, where $v_j(\omega) = 0$ for $\omega > \omega_{\max}$, with a UV cutoff $\omega_{\max}$ chosen to be much larger than all other energy scales of the problem. In the intermediate region, $0 < \omega < \omega_{\max}$, $v_j(\omega)$ is taken to be flat and equal to 1 except for a smoothing of the edges. We have checked that all physical conclusions do not critically depend on the specific choice of the UV cutoff, $\omega_{\max}$, and on the details of the smoothing [21].

For a sufficiently weak coupling to the baths [22], the dissipation superoperators for $j = \{\text{cav}, fe\}$ can be written in the temporally local form

$$\mathcal{L}_j[\rho] = \Gamma_j \{\hat{U}_j \rho \hat{S}_j + \hat{S}_j \rho \hat{U}_j^{\dagger} - \hat{S}_j \hat{U}_j \rho - \rho \hat{U}_j^{\dagger} \hat{S}_j\}, \quad (5)$$

where the system-bath interaction operators have the forms

$$\hat{S}_{fe} = |e\rangle\langle f| + |f\rangle\langle e|, \quad (6)$$

$$\hat{S}_{\text{cav}} = \hat{a}^{\dagger} + \hat{a}, \quad (7)$$

and the $\hat{U}_j$ operators take into account the non-Markovian nature of the dissipation baths. The $\hat{U}_j$ operators have a simple definition,

$$\hat{U}_j = \int_0^{\infty} d\tau\, v_j(\tau)\, e^{-i\hat{H}\tau}\, \hat{S}_j\, e^{i\hat{H}\tau}, \quad (8)$$

in terms of the bath correlation function, that is, the Fourier transform of the frequency-dependent density of states of the baths,

$$v_j(\tau) = \frac{1}{2\pi} \int_{-\infty}^{\infty} d\omega\, e^{-i\omega\tau}\, v_j(\omega). \quad (9)$$

As a result, the decay from the $|\text{in}\rangle$ to the $|\text{fin}\rangle$ eigenstate of the dressed system occurs at a frequency-dependent rate of

$$\Gamma(\text{in} \to \text{fin}) = \Gamma_j\, |\langle \text{fin}|S_j|\text{in}\rangle|^2\, v(\omega_{\text{in}} - \omega_{\text{fin}}), \quad (10)$$

and unphysical processes where the system would increase in energy ($\omega_{\text{fin}} > \omega_{\text{in}}$) upon a dissipative event are indeed forbidden.

III. THE QUANTUM VACUUM RADIATION

Once the steady-state solution ρ_{SS} of the master equation (3) has been numerically calculated [23], it is straightforward to obtain the expectation value of all one-time operators of the system in the stationary state, in particular the full photon number distribution in the cavity. However, as was pointed out in Ref. [8], this is not enough to determine the actual light emission from the system.

To distinguish real radiation from the virtual photons that are present even in the ground state of the cavity, one has in fact to evaluate the full spectral distribution of the emitted radiation [20], which is the Fourier transform of the two-time correlation function [24]

$$G_j(\omega) = \Gamma_j\, v_{\text{cav}}(\omega) \int_{-\infty}^{\infty} d\tau\, e^{i\omega\tau} \langle \hat{S}_j(t+\tau)\, \hat{S}_j(t)\rangle \quad (11)$$

for $j = \{\text{cav}, fe\}$, from which the total emission intensities I_j are obtained after integration over ω,

$$I_j = \int \frac{d\omega}{2\pi}\, G_j(\omega). \quad (12)$$

Plots of $I_{\text{cav},fe}$ as a function of Ω_{eg} are shown in Figs. 1(b) and 1(c).

Both emissions have a negligible value [25] for low Rabi frequencies $\Omega_{eg} < \omega_{\text{cav}}/2$. The first threshold occurs at $\Omega_{eg} = \omega_{\text{cav}}/2$. A second, more pronounced threshold is apparent at $\Omega_{eg} = \omega_{\text{cav}}$ and is followed by additional structure in I_{cav} for larger Ω_{eg}'s, in particular, two peaks at $\Omega_{eg} = \omega_{\text{cav}}$ and $2\omega_{\text{cav}}$. When the emitter-cavity coupling Ω_{cav} is reduced, the emission in between the two thresholds $\omega_{\text{cav}}/2 < \Omega_{eg} < \omega_{\text{cav}}$ is suppressed, as well as the intensity of the two peaks at $\Omega_{eg} = \omega_{\text{cav}}$ and $2\omega_{\text{cav}}$. These features completely disappear when the emitter is no longer coupled to the cavity [$\Omega_{\text{cav}} = 0$, red dashed line in Fig. 1(b)]. On the other hand, the upper threshold at $\Omega_{eg} = \omega_{\text{cav}}$ and the height of the plateau in the $\Omega_{eg} > \omega_{\text{cav}}$ region are almost unaffected by a variation of Ω_{cav}.

A physical explanation of these numerical observations is obtained by looking at the level schemes of the optically dressed system that are shown in Figs. 2(a) and 2(d). For $\Omega_{eg} < \omega_{\text{cav}}/2$, the dynamics of the system is limited to the subspace spanned by the two lowest energy eigenstates $|g,0\rangle \pm |e,0\rangle$ at energies $\mp\hbar\Omega_{eg}$. For $\Omega_{eg} > \omega_{\text{cav}}/2$, the energy of the $|gn\rangle - |en\rangle$ dressed states starts exceeding the energy of the $|g(n+1)\rangle + |e(n+1)\rangle$ state, which activates a family of decay processes indicated by the blue solid arrows in Fig. 2(a). These decays occur via spontaneous emission on the $e \to f$ transition, the matrix element being provided by the weak admixture (proportional to $\Omega_{\text{cav}}/\Omega_{eg}$) of the neighboring $|fn\rangle$ state via the emitter-cavity coupling Ω_{cav}. As a result, population is transferred to the upper manifolds, and significant emission intensities $I_{\text{cav},fe}$ appear as the dressed system slides back toward the lower manifolds. The second, stronger threshold that is visible in Figs. 1(b) and 1(c) at $\Omega_{eg} = \omega_{\text{cav}}$ is due to the direct $e \to f$ spontaneous decay channel that opens

up as soon as the $|gn\rangle + |en\rangle$ state exceeds in energy the $|fn\rangle$ state.

This interpretation of the thresholds is confirmed by the plots of the frequency-resolved emission spectra $G_{\rm cav}(\omega)$ and $G_{fe}(\omega)$ shown in Figs. 2(b) and 2(c). Note that, in contrast to the previous discussion of the $e \to g$ emission, the frequency ω in $G_{{\rm cav},fe}(\omega)$ corresponds to the actual physical frequency of the emitted light. The central peak at $\omega \simeq \omega_{\rm cav}$ corresponds to transitions between dressed states that only differ by the number n of cavity photons. The lateral peaks originate from transitions between different dressed states, for example, at $\omega \simeq 2\Omega_{eg} - \omega_{\rm cav}$ ($|gn\rangle - |en\rangle \to |g(n+1)\rangle + |e(n+1)\rangle$, solid blue arrows) and $\omega \simeq \omega_{\rm cav} \pm \Omega_{eg}$ ($|fn\rangle \to |gn\rangle \pm |en\rangle$, dashed and dotted red arrows). Correspondingly to each arrow in the diagram (a), the vertical lines in the spectra (b,c) indicate the expected position of the peak: the agreement with the numerical spectra is excellent.

Similar reasonings can be used to explain the peaks that are apparent in Figs. 1(b) and 1(c) around $\Omega_{eg} = \omega_{\rm cav}, 2\omega_{\rm cav}$: The stronger one at $\Omega_{eg} \simeq 2\omega_{\rm cav}$ originates from the resonant mixing of the $|g0\rangle - |e0\rangle$ and $|f1\rangle$ states by the anti-RWA terms of the emitter-cavity coupling [see the horizontal arrow in Fig. 2(d)]. The peaks at $\omega_{\rm cav} \pm \Omega_{\rm cav}/\sqrt{2}$ in the frequency-resolved spectra of Figs. 2(e) and 2(f) indeed correspond to transitions to and from the new eigenstates in the form of linear combinations of the $|g0\rangle - |e0\rangle$ and $|f1\rangle$ states. The interpretation of the weaker and narrower peak at $\Omega_{eg} \simeq \omega_{\rm cav}$ in Figs. 1(b) and 1(c) is similar: When $\Omega_{eg} \simeq \omega_{\rm cav}$, the $|g0\rangle - |e0\rangle$ and $|g2\rangle + |e2\rangle$ states are resonant and their (weaker) mixing can occur via the intermediate, nonresonant $|f1\rangle$ state.

The peak around $\Omega_{eg} = 2\omega_{\rm cav}$ has a simple physical interpretation in terms of a quantum vacuum emission process analogous to the DCE: Under the effect of the driving laser, the atom performs Rabi oscillations on the $g \leftrightarrow e$ transition, so that the atom-cavity coupling is periodically switched on and off at frequency $2\Omega_{eg}$ [19] and periodically modulates the effective optical length of the cavity. In turn, this periodic modulation is responsible for the conversion of the zero-point fluctuations of the cavity field into observable radiation [6–14], a process which, as usual, is most effective when the modulation frequency is close to a multiple of the cavity frequency [4].

While it is physically apparent that the energy that is emitted by the system as quantum vacuum radiation comes at the expense of the laser beam driving the $g \leftrightarrow e$ Rabi oscillations, understanding the physics on the dressed-level scheme of Fig. 2(d) requires a bit more attention. The dissipative processes responsible for the emission of quantum vacuum radiation make the system slide down on the dressed-level scheme. This downward drift is compensated by $e \to g$ spontaneous emission processes where the system is brought up again on the dressed-level scheme by emitting photons at a frequency lower than the drive laser one ω_L.

IV. THE BACK-REACTION EFFECT

After this lengthy preparatory discussion, we are finally in a position to illustrate the main result of this work, namely the back-reaction effect of the quantum vacuum onto the drive beam. To this purpose, the simplest quantity to consider is the absorption of the drive laser light by the emitter when this is excited on the $g \to e$ transition.

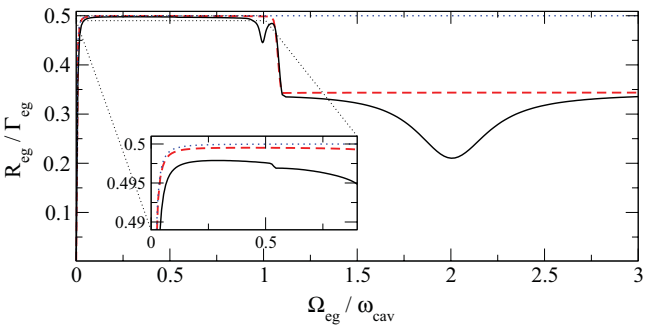

FIG. 3. (Color online) Solid line: Rate of photon absorption from the drive laser as a function of its Rabi frequency Ω_{eg}. Same system parameters as in Fig. 1. Red dashed line: same curve in the vanishing emitter-cavity coupling case $\Omega_{\rm cav} = 0$. Blue dotted line: same curve for a two-level emitter.

Using standard results of quantum optics [20], the average rate of photon absorption is related to the imaginary part of the expectation value of the emitter polarization by

$$R_{eg} = 2\Omega_{eg}\,{\rm Im}\{{\rm Tr}[\hat{c}^{\dagger}_{eg}\,\rho_{SS}]\}. \tag{13}$$

A plot of this quantity as a function of Ω_{eg} is shown in Fig. 3. For low Ω_{eg}, the dependence is the standard one of saturated absorption by a two-level atom (blue dotted line). At larger values of Ω_{eg}, two sudden downward jumps are observed at $\Omega_{eg} = \omega_{\rm cav}/2$ and (more visibly) at $\Omega_{eg} = \omega_{\rm cav}$: Both these jumps are closely related to the thresholds previously observed in $I_{\rm cav}$ and I_{fe}.

Clear signatures of the back-reaction effect are visible as dips in the absorption spectrum around $\Omega_{eg} = \omega_{\rm cav}$ and $\Omega_{eg} = 2\omega_{\rm cav}$. Both the position and the linewidth of the absorption dips perfectly match the corresponding peaks in the quantum vacuum emission spectrum shown in Fig. 1: When the emission intensity is the largest, the emitter experiences the strongest friction force opposing to the Rabi oscillations between the g and the e state, which in turn results in a significant suppression of the absorption rate experienced by the drive laser [26].

The interpretation of the dips in terms of back-reaction effect of the quantum vacuum is further validated by the observation that their strength decreases when the emitter-cavity coupling $\Omega_{\rm cav}$ is reduced and finally completely disappears for $\Omega_{\rm cav} = 0$ (red dashed line in Fig. 3). Remarkably, the amplitude of both peaks is a non-negligible fraction of the total absorption rate by the emitter, which confirms the promise of our optical detection proposal.

V. CONCLUSIONS

In conclusion, we have developed a theoretical model to study the optical properties of a three-level emitter embedded in an optical microcavity beyond the rotating-wave approximation: Rabi oscillations under the effect of a drive laser result in a sizable emission of quantum vacuum radiation. Experimentally accessible signatures of the back-reaction effect of the quantum vacuum appear as marked dips in the absorption

spectrum of the drive beam. Drawing an analogy with the dynamical Casimir effect, these peaks can be interpreted as due to the optical analog of the mechanical friction force exerted by the quantum vacuum onto a nonuniformly accelerated mirror.

ACKNOWLEDGMENTS

I.C. is grateful to R. Balbinot, A. Fabbri, D. Faccio, M.-T. Jaekel, A. Lambrecht, S. Reynaud, and S. Savasta for continuous discussions. I.C. acknowledges financial support from ERC through the QGBE grant.

[1] P. W. Milonni, *The Quantum Vacuum: An Introduction to Quantum Electrodynamics* (Academic Press, San Diego, CA, 1993).

[2] N. D. Birrell and P. C. W. Davies, *Quantum Fields in Curved Space* (Cambridge University Press, Cambridge, 1982).

[3] G. T. Moore, J. Math. Phys. **11**, 2679 (1970); S. A. Fulling and P. C. W. Davies, Proc. R. Soc. London A **348**, 393 (1976); P. C. W. Davies and S. A. Fulling, *ibid.* **356**, 237 (1977).

[4] A. Lambrecht, J. Opt. B **7**, S3 (2005).

[5] M. Kardar and R. Golestanian, Rev. Mod. Phys. **71**, 1233 (1999); M.-T. Jaekel and S. Reynaud, Quantum Opt. **4**, 39 (1992); W. Barton and C. Eberlein, Ann. Phys. **227**, 222 (1993).

[6] E. Yablonovitch, Phys. Rev. Lett. **62**, 1742 (1989).

[7] V. V. Dodonov, A. B. Klimov, and D. E. Nikonov, Phys. Rev. A **47**, 4422 (1993); C. K. Law, *ibid.* **49**, 433 (1994); M. Artoni, A. Bulatov, and J. Birman, *ibid.* **53**, 1031 (1996).

[8] C. Ciuti, G. Bastard, and I. Carusotto, Phys. Rev. B **72**, 115303 (2005); C. Ciuti and I. Carusotto, Phys. Rev. A **74**, 033811 (2006); S. De Liberato, C. Ciuti, and I. Carusotto, Phys. Rev. Lett. **98**, 103602 (2007).

[9] C. Braggio, G. Bressi, G. Carugno, C. Del Noce, G. Galeazzi, A. Lombardi, A. Palmieri, G. Ruoso, and D. Zanello, Europhys. Lett. **70**, 754 (2005).

[10] I. Carusotto, M. Antezza, F. Bariani, S. De Liberato, and C. Ciuti, Phys. Rev. A **77**, 063621 (2008).

[11] S. De Liberato, D. Gerace, I. Carusotto, and C. Ciuti, Phys. Rev. A **80**, 053810 (2009); J. R. Johansson, G. Johansson, C. M. Wilson, and F. Nori, Phys. Rev. Lett. **103**, 147003 (2009).

[12] F. X. Dezael and A. Lambrecht, Europhys. Lett. **89**, 14001 (2010).

[13] D. Faccio and I. Carusotto, Europhys. Lett. **96**, 24006 (2011).

[14] C. M. Wilson, G. Johansson, A. Pourkabirian, M. Simoen, J. R. Johansson, T. Duty, F. Nori, and P. Delsing, Nature (London) **479**, 376 (2011).

[15] G. Günter, A. A. Anappara, J. Hees, A. Sell, G. Biasiol, L. Sorba, S. De Liberato, C. Ciuti, A. Tredicucci, A. Leitenstorfer, and R. Huber, Nature (London) **458**, 178 (2009).

[16] J. M. Raimond, M. Brune, and S. Haroche, Rev. Mod. Phys. **73**, 565 (2001).

[17] A. Wallraff, D. I. Schuster, A. Blais, L. Frunzio, R.-S. Huang, J. Majer, S. Kumar, S. M. Girvin, and R. J. Schoelkopf, Nature (London) **431**, 162 (2004).

[18] K. Hennessy, A. Badolato, M. Winger, D. Gerace, M. Atatüre, S. Gulde, S. Fält, E. L. Hu, and A. Imamoğlu, Nature (London) **445**, 896 (2007).

[19] A. Ridolfo, R. Vilardi, O. Di Stefano, S. Portolan, and S. Savasta, Phys. Rev. Lett. **106**, 013601 (2011).

[20] C. W. Gardiner and P. Zoller, *Quantum Noise* (Springer-Verlag, Berlin, 2004).

[21] In the numerics, the $v_j(\omega)$'s have been smoothed with a Gaussian tail of width $\Delta\omega = 0.025\omega_{\rm cav}$ past the extrema at $\omega_{\rm edge} = 0.1\omega_{\rm cav}$ and $\omega_{\rm max} = 21\omega_{\rm cav}$.

[22] H.-P. Breuer and F. Petruccione, *The Theory of Open Quantum Systems* (Clarendon Press, Oxford, UK, 2006).

[23] In our numerical calculations, we consider the right-hand side of (3) as a linear operator on the space of density matrices. The steady-state $\rho_{\rm SS}$ corresponds to an eigenvector of this operator with a zero eigenvalue and can be found using standard linear algebra numerical packages.

[24] The two-time averages are defined as usual as $\langle A(t+\tau)B(t)\rangle = {\rm Tr}[A\rho'(t+\tau)]$, where $\rho'(t+\tau)$ is the solution of (3) starting from the initial condition $\rho'(t) = B\rho(t)$. This definition of course holds only for $\tau > 0$ but can be straightforwardly extended to $\tau < 0$ using the formula $\langle A(t+\tau)B(t)\rangle = \langle B^\dagger(t)A^\dagger(t+\tau)\rangle^*$.

[25] The nonvanishing values of $I_{{\rm cav},fe}$ down to $\Omega_{eg} = 0$ are an artifact of the weak-coupling approximation to write the master equation in the temporally local form (3).

[26] A similar phenomenon occurs in a resonantly driven harmonic oscillator, where the absorbed energy for a given driving strength scales inversely with the damping rate.